Excessive serine from the bone marrow microenvironment impairs megakaryopoiesis and thrombopoiesis in Multiple Myeloma

Wen Zhou (wenzhou@csu.edu.cn)
Cancer Research Institute, School of Basic Medical Sciences, Central South University

Chunmei Kuang
Cancer Research Institute, School of Basic Medical Sciences, Central South University

Meijuan Xia
Institute of Hematology & Blood Diseases Hospital, Chinese Academy of Medical Science & Peking Union Medical College

Gang An
Institute of Hematology and Blood Disease Hospital,CAMS & PUMC

Cuicui Liu
State Key Laboratory of Experimental Hematology, Institute of Hematology & Blood Diseases Hospital, Chinese Academy of Medical Sciences & Peking Union Medical College

Jingyu Zhang
Cancer Research Institute, School of Basic Medical Sciences, Central South University

Zhenhao Liu
Xiangya Hospital, Central South University https://orcid.org/0000-0003-4465-5925

Cong Hu
Cancer Research Institute, School of Basic Medical Sciences, Central South University

Bin Meng
Cancer Research Institute, School of Basic Medical Sciences, Central South University

Pei Su
State Key Laboratory of Experimental Hematology, Institute of Hematology & Blood Diseases Hospital, Chinese Academy of Medical Sciences & Peking Union Medical College

Jiliang Xia
University of South China

Jiaojiao Guo
Cancer Research Institute, School of Basic Medical Science, Central South University, Changsha 410078, China.

Yinghong Zhu
Cancer Research Institute, School of Basic Medical Sciences, Central South University

Xuan Wu

Cancer Research Institute, School of Basic Medical Sciences, Central South University

Yi Shen

Department of Orthopaedic Surgery, Second Xiangya Hospital, Central South University

Xiangling Feng

Xiangya School of Public Health, Central South University

Yanjuan He

Department of Hematology, Xiangya Hospital, Central South University

Jian Li

Peking Union Medical College Hospital, Chinese Academy of Medical Sciences & Peking Union Medical College https://orcid.org/0000-0002-4549-0694

Lugui Qiu

Institute of Hematology and Blood Diseases Hospital, Chinese Academy of Medical Sciences & Peking Union Medical College https://orcid.org/0000-0002-8752-0644

Jiaxi Zhou

Institute of Hematology and Blood Diseases Hospital, Chinese Academy of Medical Sciences and Peking Union Medical College

---

Article

Keywords: Multiple Myeloma, Thrombocytopenia, Serine, SVIL

Posted Date: May 2nd, 2022

DOI: https://doi.org/10.21203/rs.3.rs-1572144/v1

Excessive serine from the bone marrow microenvironment impairs megakaryopoiesis and thrombopoiesis in Multiple Myeloma

Chunmei Kuang[1,2#], Meijuan Xia[3#], Gang An[3], CuiCui Liu[3], Jingyu Zhang[1,2], Zhenhao Liu[1,2], Cong Hu[1,2], Bin Meng[1,2], Pei Su[3], Jiliang Xia[1,2], Jiaojiao Guo[1,2], Yinghong Zhu[1,2], Xuan Wu[1,2], Yi Shen[4], Xiangling Feng[5], Yanjuan He[1], Jian Li[6], Lugui Qiu[3], Jiaxi Zhou[3*], Wen Zhou[1,2*]

[1]State Key Laboratory of Experimental Hematology, Key Laboratory of Carcinogenesis and Cancer Invasion, Ministry of Education; Key Laboratory of Carcinogenesis, National Health and Family Planning Commission, Department of Hematology, Xiangya Hospital, Central South University, Changsha, Hunan, China

[2]Cancer Research Institute, School of Basic Medical Science, Central South University, Changsha, Hunan, China

[3]State Key Laboratory of Experimental Hematology, National Clinical Research Center for Blood Diseases, Chinese Academy of Medical Sciences & Peking Union Medical College, Tianjin, China

[4]Department of Orthopaedic Surgery, Second Xiangya Hospital, Central South University, Changsha, Hunan, China

[5]Xiangya School of Public Health, Central South University, Changsha, Hunan, China

[6]Department of Hematology, Peking Union Medical College Hospital, Chinese Academy of Medical Sciences and Peking Union Medical College, Beijing, China

#These authors contributed equally to this study; *Correspondence: wenzhou@csu.edu.cn, zhoujx@ihcams.ac.cn.

Running title: Serine Impaired thrombopoiesis in MM

Key points: 1. Thrombocytopenia predicts the worst survival in the MM patients;

2. Elevation of serine in BMME contributes to thrombocytopenia;

3.Inhibiting serine utilization and intake restores thrombocytopenia.

Text word count: 9836; number of figures: 7; number of references: 46; number of Supplementary figures: 6; number of Supplementary Material and Methods: 1; number of Supplementary tables: 8

Abstract

Thrombocytopenia is a major complication in a subset of patients with multiple myeloma (MM). However, little is known about its development and significance during MM. Here, we show that thrombocytopenia is linked to poor prognosis in the MM patients. In addition, we identify serine, which is released from MM cells into the bone marrow microenvironment (BMME), serves as a key metabolic factor that suppresses megakaryopoiesis and thrombopoiesis and eventually causes the thrombocytopenia. The impact of excessive serine on thrombocytopenia is mainly mediated through the suppression of megakaryocyte (MK) differentiation in the BM and the induction of apoptosis of platelets in the peripheral blood (PB). At the molecular level, the extrinsic serine molecules are transported into MKs through the channel protein SLC38A1 and downregulates the actin-binding protein Supervillin (SVIL) via S-adenosyl-methionine (SAM)-mediated tri-methylation of H3K9, ultimately leading to the impairment of megakaryopoiesis as well as thrombopoiesis. Inhibition of serine utilization or the treatment with thrombopoietin (TPO) enhances megakaryopoiesis and thrombopoiesis and suppresses MM progression. Together, we identify serine as a key metabolic regulator of thrombocytopenia in MM, unveil novel molecular mechanisms governing MM progression, and provide potential new therapeutic strategies for treating MM patients by targeting thrombocytopenia.

Key words: Multiple Myeloma; Thrombocytopenia; Serine; SVIL

Introduction

Multiple myeloma (MM) is the second most common hematologic malignancy with high incidence and mortality rates [1]. Clonal proliferation of malignant plasma cells within the BMME results in a host of clinical manifestations including hypercalcemia, renal failure, lytic bone lesions, and anemia, infection and bleeding induced by cytopenia [2]. Thrombocytopenia has also been observed in patients with MM, although it is a relatively less common complication [3-6]. The incidence of thrombocytopenia and its significance in the development of MM are still poorly defined.

In the bone marrow (BM), the cells of the megakaryocytic lineage are originated from hematopoietic stem/progenitor cells (HSPCs) and undergo differentiation, ultimately leading to the formation of platelets [7]. It has been reported that thrombocytopeniais caused by diminished HSPCs in the BM, defective megakaryocyte differentiation, unfavorable BMME, and/or immune-mediated platelet apoptosis [8-11]. Recently, we demonstrated that the intestinal bacteria promote MM progression by elevating the level of BM glutamine and phosphoglycerate dehydrogenase (PHGDH), the first rate-limiting enzyme of the serine synthesis pathway (SSP) and that glutamine enhances cell proliferation and BTZ resistance of MM by increasing GSH synthesis in MM cells [12,13]. Thus, the alterations of metabolite levels in the BMME can accelerate MM. It has also been shown that metabolites such as cholesterol and serotonin are involved in megakaryopoiesis and thrombopoiesis during HSPC differentiation, suggesting that the intake of metabolites might play a role in MK differentiation [14,15]. However, whether MK differentiation and platelet production from HSPCs are impaired in MM and what metabolites are involved in these processes remain to be defined.

In the present study, we determined the clinical impact of thrombocytopenia in patients with MM at diagnosis. We also examined the differential metabolites in the BMME of MM patients with thrombocytopenia and the effects of metabolites on megakaryopoiesis and thrombopoiesis. We further investigated the role and the molecular mechanism by which thrombocytopenia is induced by metabolites. Finally, we explored the therapeutic potential of intervening metabolite intake in preventing thrombocytopenia.

Results

Thrombocytopenia is linked to poor prognosis in MM patients

To investigate the platelet counts and their potential correlation with disease progression in newly diagnosed MM (NDMM) patients, we studied 1,468 patients and classified them into three groups based on the platelet counts in the peripheral blood (PB) at the time of diagnosis. The criterion of thrombocytopenia was defined as an absolute platelet count $\leq 100\times10^9$/L in PB according to previous studies [16], while elevated platelet counts were defined as those higher than the upper limit of the normal count. Three groups were stratified as follows: normal platelet counts (100-300$\times10^9$/L), high platelet (>300$\times10^9$/L) and low platelet counts ($\leq$100$\times10^9$/L). Among those patients, 1,041 (70.9%) had normal platelet counts, while 311 (21.2%) and 116 patients (7.9%) had low and high platelet counts, respectively (Fig. 1a).

We next compared the clinicopathologic parameters among the three groups, including gender, age, ISS (International Staging System) stage, DS (Durie -Salmon) stage, percentages of plasma cells, renal dysfunction, serum lactate dehydrogenase (LDH), serum calcium and IgH translocations, to explore whether platelet counts correlated with disease progression and may

serve as a prognostic marker in MM patients. We found that platelet counts had no correlation with gender, age, renal dysfunction, serum LDH, serum calcium and IgH translocations (Table 1). Intriguingly, we observed strong correlation between the platelet numbers and ISS stage, as evidenced by the significant difference in platelet counts in patients among three different stages. Specifically, the patients in stage I had the highest number of platelets, while the patients in stage III showed the lowest platelet count (Fig. 1b). Moreover, this correlation may be explained by the increased proportion of MM patients with thrombocytopenia at the stage III of ISS (Supplementary Fig. 1a). In addition, we found that the platelet counts were also associated with DS stage ($p = 0.002$), the percentage of plasma cells in BM ($p < 0.001$), the level of hemoglobin (Hb) ($p < 0.001$), 1q21 gain ($p = 0.004$) and TP53 deletion ($p = 0.037$) (Table 1).

To further assess whether platelet counts were associated with OS and PFS, we conducted Kaplan-Meier analysis of the MM patients. Although the risk stratification of MM is widely available in the clinics [17], we found that both OS and PFS were significantly worsened once the platelet counts were lower than 100×10^9/L. In contrast, no difference for OS and PFS was observed between patients with platelet count higher than $300x10^9$/L and those within 100-$300x10^9$/L (Supplementary Fig. 1b). We next performed multivariable Cox regression analysis to investigate the prognostic value of platelet counts in MM patients. We found that platelet counts, and 1q21 gain and TP53 deletion are independent prognostic factors for MM patients (Supplementary Table S1). We further combined the analysis of platelet count with the ISS stages. Not surprisingly, platelet counts showed minimal correlation with OS or PFS in patients at stage I. However, both OS and PFS were significantly shorter when the platelet count was

lower than 100×10^9/L in patients of stage II and III (Supplementary Fig. 1c). To analyze the patients with lower platelet counts, we divided them into two groups with platelet counts 50-100×10^9/L and $<50\times10^9$/L, respectively. Strikingly, we found that patients with $< 50\times10^9$/L platelet counts exhibited extremely inferior OS and PFS when compared with those with normal platelet counts. The most significant difference was observed in stage III MM patients (Fig. 1c, d). Thus, consistent with previous observations, the lower platelet count (or thrombocytopenia) is tightly linked to the progression and the outcome of MM. We also demonstrated that the lowest platelet count ($< 50\times10^9$/L) predicts the poorest OS and PFS. Thus, low platelet counts may be used as a marker for unfavorable outcomes for MM patients.

It is well known that MKs are originated from HSPCs and MKs extend long branching processes into sinusoidal blood vessels to release platelets within the BM. It is therefore possible that MKs may be also impaired during MM progression and cause the reduction in platelet counts. We thus examined the number of MKs in MM patients of different stages or with various platelet counts, leading us to discover a gradual decrease of MK numbers in MM patients compared with the healthy donors (Supplementary Table S2). Specifically, the patients at stage II and III showed significantly lower amounts of MKs (Fig. 1e). Furthermore, fewer MKs were found in the patients with lower count of platelets, and the number of MKs and platelets correlated positively ($n = 121$, $r = 0.2868$, $p = 0.0014$) (Fig. 1f, g). Thus, megakaryopoiesis is also impaired in MM patients.

We further examined the dynamic changes of platelet counts during MM progression *in vivo* by taking advantage of a previously described MM mouse model [13,18]. We measured complete blood counts every week after the injection of 5TGM1-luc cells. MM progression in the mice

was monitored weekly via the determination of tumor burden, including bioluminescent imaging, and the concentration of serum IgG2b (Fig. 1h). As expected, increased tumor infiltration and gradual elevation of serum IgG2b level were observed during the progression of MM (Supplementary Fig. 1d and Fig. 1i). Interestingly, the gradual decrease of platelets was seen in parallel with the elevation of serum IgG2b level (Fig. 1i). Moreover, platelet counts correlated strongly with IgG2b ($r = 0.52$, $p < 0.001$) (Fig. 1j).

We next measured the distributions of MKs in the BM by conducting immunostaining of CD41, a widely used MK surface marker. Indeed, much fewer $CD41^+$ MKs were observed in 5TGM1 mice than in the control mice (Fig. 1k). The number of MKs in BM was reduced during disease progression, while a striking decrease was observed when the level of IgG2b was above 6mg/mL (Supplementary Fig. 1e). In addition, the number of MKs was significantly lower in 5TGM1 mice with normal platelet counts than those with low platelet counts (Supplementary Fig. 1f, g). We also measured the number of the progenitor cells along the megakaryocytic lineages, including LSK, CMP and MEP, and observed a decrease in these MK progenitors, especially in mice with IgG2b above 6 mg/mL (Supplementary Fig. 1h). Together, analyses of MM patients and experiments with the MM mouse model suggest that megakaryopoiesis and thrombopoiesisis severely impaired and leads to thrombocytopenia during MM progression.

Serine is upregulated in the BM and linked to thrombocytopenia in MM

The production of platelets by BM MKs which are originated from HSPCs is tightly depends on their interactions with the BM niche. We therefore asked whether the defects in megakaryopoiesis and thrombopoiesis that occur in the BM of MM patients were caused by

soluble factors in the niche. To test this, we took advantage of a previously established *in vitro* culture system to model human megakaryopoiesis and thrombopoiesis [19]. We assessed MK differentiation and platelet production of HSPCs ($CD34^+$ cells) incubated with either the BM plasma associated with normal platelet counts or with low platelet counts (Fig. 2a). Interestingly, we found that the fraction of $CD41a^+CD42b^+$ cells was significantly reduced with the treatment of BM plasma of the low platelet counts ($p < 0.05$) (Fig. 2b). The formation of proplatelets and $CD41a^+CD42b^+$ platelet-like particles (PLPs) was also significantly impaired with the treatment of BM plasma of low platelet counts ($p < 0.001$) (Fig. 2c, d).

Recently, we have validated that gut microbiome and PHGDH promotes MM progression via de novo synthesis of glutamine and serine, respectively [13]. To identify the potential metabolic factor(s) that mediate the inhibitory effects of myeloma cells, we first conducted untargeted metabolomics analysis of the BM plasma collected from the MM patients using chromatography-mass spectrometry. We detected approximately 200 metabolites that cover a wide range of the metabolic pathways. Among those, 16 metabolites, including both amino acids and lipids, exhibited significant differences between patients with normal platelet counts (platelet count 120-300) and low platelet counts (Fig. 2e). Interestingly, 5 amino acids (glycine, L-serine, L-aspartic acid, L-glutamic acid and ornithine) were found to accumulate more in patients with lower platelet counts (Fig. 2f). To gain further insights into the changes of metabolites, we determined the levels of amino acids by using Liquid Chromotography Mass Spectrometry and found that the levels of glycine, L-serine, L-glutamic acid, and ornithine were much higher in the BM of patients with low platelet counts (Fig. 2g, h). We also measured the level of the 4 amino acids in the plasma of the BM in 5TGM1 and control mice, allowing us to

187 discover that the levels of glycine, L-serine and ornithine were higher in 5TGM1 mice. In
188 contrast, L-glutamic acid exhibited no significant difference between the two groups
189 (Supplementary Fig. 2a).

190 We next asked whether the 4 amino acids impacted megakaryopoiesis and thrombopoiesis
191 *in vitro.* We treated $CD34^+$ cells with these amino acids individually using the MK
192 differentiation system as described earlier in this study. While glycine and L-glutamic acid
193 exerted minimal effects on megakaryopoiesis and/or partial effects on thrombopoiesis, serine
194 and ornithine potently suppressed megakaryopoiesis and thrombopoiesis, with serine exhibiting
195 the most significant effect (Supplementary Fig. 2b-d). Together, experiments with metabolic
196 profiling and functional validation allowed us to reveal serine as a potential key factor in the
197 BM microenvironment to control megakaryopoiesis and thrombopoiesis.

198

199 **Serine inhibits megakaryopoiesis and thrombopoiesis both *in vitro* and *in vivo***

200 We next determined whether serine functioned to suppress megakaryopoiesis and
201 thrombopoiesis. First, we added increasing concentrations of serine to the MK differentiation
202 system *in vitro*, which led to elevating levels of intracellular serine in the cells, suggesting that
203 the intake of extracellular serine of MKs was dose-dependent (Supplementary Fig. 3a). We then
204 discovered that at the serine dose of 2 mM, MK differentiation and platelet generation were
205 inhibited, while minimal effects were seen when serine was under 0.5 mM. At 8 mM of serine,
206 the inhibition was highly potent (Fig. 3a-c).

207 We also assessed the kinetic pattern of serine levels (in week 0, 3 and 6) in the PB serum of
208 5TGM1 mice *in vivo*. Consistent with the reduced platelet counts in 5TGM1 mice in week 6,

209 the level of serine was higher in PB serum of the 5TGM1 mice than the control mice, while
210 little difference was observed in 5TGM1 and control mice in week 3 (Supplementary Fig. 3b).
211 Furthermore, the concentration of serine in the serum correlated inversely with platelet counts
212 (Supplementary Fig. 3c).

213 After assessing the function of serine using the *in vitro* assay, we further elucidated its effects
214 *in vivo*. We developed MM in mice by injecting 5TGM1 cells and then fed them with diets with
215 or without serine (Fig. 3d). The two diets caused significant differences in the level of serine *in*
216 *vivo*. After the depletion of serine from the diet, the level of serine in PB serum clearly
217 decreased (Supplementary Fig. 3d). We further measured the dynamic changes of tumor cells
218 *in vivo* to monitor the tumor burden. We found that the number of infiltrated tumor cells was
219 smaller in mice with serine-deficient diet than the control mice ($p < 0.05$) (Fig. 3e, f). We then
220 compared the level of IgG2b in mice with or without the serine diet. While minor difference in
221 IgG2b level was observed after 3 weeks of diet, the difference became quite significant after 5
222 weeks of intake (Fig. 3g). Consistent with the results from the *in vitro* experiments, the platelet
223 count in the mice fed with serine-deficient diet was sustained at a higher level, and the
224 deprivation of serine intake indeed prevented the decrease of platelets during MM progression
225 ($p < 0.05$) (Fig. 3h). Finally, we found that the deprivation of serine from the diet significantly
226 extended the survival time ($p < 0.05$) (Fig. 3i). Thus, the limitation of serine intake suffices to
227 delay MM progression *in vivo*.

228 It was previously reported that an increased apoptotic rate of platelets is another cause of
229 thrombocytopenia [20,21]. These findings prompted us to determine whether the rate of platelet
230 apoptosis was elevated in MM patients. We incubated platelets with the PB serum from either

231 healthy donors or MM and found that the rate of apoptosis was significantly higher in platelets
232 incubated with the serum from MM ($p < 0.05$) (Fig. 3j). These findings suggest the existence
233 of pro-apoptotic factors in the serum of MM patients. In separate experiments, we also
234 confirmed the increase of serine levels in the serum of MM patients using targeted metabolic
235 analysis ($p < 0.05$) (Fig. 3k). Furthermore, the addition of serine enhanced platelet apoptosis,
236 as indicated by the flow cytometry analysis (Supplementary Fig. 3e, f).
237 At the molecular level, we found that serine increased caspase3 cleavage and enhanced the
238 expression of p53 and BAD, while reducing the BCL-xL level in platelets isolated from healthy
239 donors and control mice (Fig. 3l). Moreover, MM patients with high levels of serine and
240 thrombocytopenia were associated with ISS stage, % plasma cells in the BM, the levels of Hb
241 and calcium (Supplementary Table S3). Thus, high levels of serine induce apoptosis of platelets
242 in MM.
243
244 **Serine intake is mediated by SLC38A1**
245 To explore the potential downstream target genes of serine, we performed RNA-sequencing
246 analysis of$CD34^+$ cells treated with vehicle or serine and found that a total of 3,247 genes were
247 upregulated while 2,002 were downregulated in cells treated with serine (Supplementary Table
248 S4). Among those, SLC38A1, MTHFD1L, GCSH and PHGDH were upregulated (Fig. 4a),
249 suggesting that exogenous serine might induces alterations in serine transport, conversion of
250 serine to glycine, folate cycle, and serine synthesis (Fig. 4b). Furthermore, SLC38A1
251 upregulation was confirmed with RT-PCR analysis (Fig. 4c). To explore whether the intake of
252 exogenous serine is mediated by the amino transporter, we depleted SLC38A1 by using

shRNAs in $CD34^+$ cells via lentiviral infection, leading to the reduction of serine levels in the conditioned medium (CM) from cells with SLC38A1 knockdown (Supplementary Fig. 4a; Fig. 4d, e). Furthermore, knockdown of SLC38A1 enhanced megakaryocytic differentiation (Fig. 4f) and PLP generation (Fig. 4g, h). Thus, SLC38A1 serves as a critical transporter mediating the inhibitory effects of serine on megakaryopoiesis and thrombopoiesis. Restriction of serine intake may therefore serve as a potential effective strategy for improving thrombocytopenia.

Serine downregulates Supervillin via S-adenosyl-methionine-mediated tri-methylation of H3K9

To further dissect the molecular mechanism by which serine regulates megakaryopoiesis and thrombopoiesis, we determined the fate of the carbons in serine. We cultured $CD34^+$ cells or MKs in media containing $^{13}C_3$-serine (Supplementary Fig. 5a) and found that serine-derived carbons were incorporated into glycine, methionine, glucose and nucleotides in cells undergoing MK differentiation (Fig. 5a and Supplementary Table S5). Because the abundance of labeled methionine was greater than other metabolites, we next measured the level of methionine upon serine treatment, leading us to find that methionine was significantly upregulated in cells treated with serine ($p < 0.05$) (Fig. 5b). Interestingly, the addition of excessive methionine also decreased megakaryocytic differentiation and PLP generation (Fig. 5c-e). Thus, serine is likely incorporated into the methionine cycle through the folate one-carbon metabolism (Fig. 5f).

Next, we analyzed the contribution of serine-dependent one-carbon metabolism to the methionine cycle and the methylation reactions in differentiated cells. We first assessed the

expression of methyltransferases and found that SETDB2 and NSD1 were significantly upregulated upon serine stimulation (Supplementary Fig. 5b). Because SETDB2 is an H3K9 methyltransferase that catalyzes H3K9-me3 to repress gene expression [22], we then examined the level of H3K9-me3 after serine and methionine stimulation. As expected, the level of SETDB2 and H3K9-me3 was elevated in cells treated with serine and methionine (Fig. 5g and Supplementary Fig. 5c).

To identify the potential methylated substrates regulated by serine, we performed assay for transposase-accessible chromatin using sequencing (ATAC-seq) in cells treated with vehicle or serine, respectively (Supplementary Table S6), allowing us to discover distinct pattern and numbers of peaks between control and serine-treated cells (Supplementary Fig. 5d). By integrating ATAC-seq and RNA-seq analyses, we identified 15 downregulated genes (Fig. 5h and Supplementary Fig. 5e), five of which were further confirmed (Supplementary Fig. 5f), including Supervillin (SVIL), SHANK3 and FRYL (Fig. 5h). To assess whether serine inhibits these genes through DNA methylation, we first examined the methylation status of the promoter by using Methylation-Specific PCR (MS-PCR). However, there was no significant difference in DNA methylation upon serine stimulation (Supplementary Fig. 5g). Because H3K9-me3 is a repressive mark that has been implicated in heterochromatin formation, we assessed the binding of H3K9-me3 to the promoter of SVIL, SHANK3 and FRYL and observed enhanced binding of H3K9-me3 to the promoter of SVIL and SHANK3 upon serine stimulation, while the binding to SVIL promoter is stronger than SHANK3 (Fig. 5i). At the functional level, depletion of SVIL and SHANK3 inhibited megakaryopoiesis and thrombopoiesis (Supplementary Fig. 5h-j), while overexpression of SVIL rescued the inhibitory effect of

297 serine-mediated thrombocytopenia (Fig. 5j). In contrast, RUNX1, a well-established regulator
298 of megakaryocyte specification, maturation, and thrombopoiesis, was downregulated in the
299 RNA-seq but not in the ATAC-seq analysis (Supplementary Fig. 5k, l). Because SETDB2 is
300 responsible for catalyzation of H3K9-me3, we then assessed the binding of H3K9-me3 to the
301 promoter of SVIL after knockdown of SETDB2 (Supplementary Fig. 5m). As expected,
302 depletion of SETDB2 rescued the enhanced binding of H3K9-me3 to the promotor of SVIL
303 mediated by serine (Supplementary Fig. 5n). Together, these results suggest that serine inhibits
304 megakaryopoiesis and thrombopoiesisvia via SVIL downregulation, which is mediated by S-
305 adenosyl-methionine (SAM)-mediated tri-methylation of H3K9.
306
307 **Serine accumulated in the BM microenvironment is released from myeloma cell**
308 How is serine accumulated in the BM microenvironment? We previously demonstrated that
309 PHGDH and PSPH catalyze the conversion of 3- phosphoglycerate to serine, leading us to
310 assess PHGDH and PSPH mRNA levels in plasma cells, HSPCs, T lymphocytes, B
311 lymphocytes and erythroid cells isolated from the BM of tumor-bearing 5TGM1 mice (Fig. 6a).
312 Strikingly, we detected much higher levels of PHGDH and PSPH mRNA in plasma cells than
313 in other niche cells (Fig. 6b), suggesting that the PHGDH was upregulated in MM cells and
314 may enhance the secretion of serine to the BM. In keeping with the notion, the fraction of
315 plasma cells positively correlated with the serine level in the serum of 5TGM1 mice
316 (Supplementary Fig. 6a). We therefore hypothesized that myeloma cells in the BM
317 microenvironment might exert the inhibitory effects on megakaryopoiesis and thrombopoiesis
318 by releasing excessive serine.

To test this hypothesis, we first determined the effects of applying the CM from MM cell culture on megakaryocyte differentiation. Interestingly, experiments with the immunofluorescence assay showed that the derivation of $CD41a^+CD42b^+$ MKs was suppressed after the incubation with the CM from three different MM cell lines including ARP1, RPMI-8226 and OPM2 (Fig. 6c). The results from the flow cytometry assay further confirmed the inhibition of megakaryocytic differentiation by the CM from MM cells (Fig. 6d). We also found that the CM severely prevented the production of proplatelets and $CD41a^+CD42b^+$ PLP particles (Fig. 6e, f). Furthermore, the megakaryocytic differentiation of C-kit^+ cells from mice was also suppressed by the CM produced from 5TGM1 cells (Supplementary Fig. 6b, c). Thus, the myeloma cells exert the inhibitory effects on megakaryopoiesis and thrombopoiesis, likely via the secretion of extrinsic factor(s).

We next directly assessed whether serine was indeed secreted from MM cells. We measured ^{13}C-labeled serine by exploring $^{13}C_2$-glycine metabolic flux of ARP1 cells and found that ^{13}C-labeled serine was gradually elevated in the CM of ARP1 cells (Fig. 6g). We then evaluate the effects of manipulating PHGDH expression on serine production, megakaryopoiesis and thrombopoiesis by generating APR1 myeloma cells with PHGDH ectopic expression or knockdown. As expected, overexpression of PHGDH increased the level of serine in the CM (Supplementary Fig. 6d), while the CM collected from PHGDH-overexpressing APR1 cells inhibited megakaryocytic differentiation and PLP generation ($p < 0.05$) (Fig. 6h-j). In contrast, knockdown of PHGDH decreased the level of serine in the CM (Supplementary Fig. 6e) and facilitated megakaryocytic differentiation and PLP derivation (Fig. 6k-m). To further investigate whether serine from MM cells affected the expression of serine metabolism-related

genes, we assessed the expression of those genes by RNA-seq analysis. Consistent with the mRNA expression profiling of serine treatment, SLC38A1, GCSH and PHGDH were upregulated in cells treated with CM of ARP1 cells (Supplementary Fig. 6f).

Megakaryopoiesis and thrombopoiesis takes place largely in the BMME with myeloma cells and thus might be affected by the potential extrinsic factors produced by MM cells. To explore this, we determined the transition of serine to methionine in MKs upon the treatment of CM produced from MM cells (Fig. 6n). Intriguingly, enhanced labeling of methionine was observed in cells treated with the CM of MM cells (Fig. 6o). Consistently, trimethylation of H3K9 was also upregulated in cells with the CM treatment (Fig. 6p). These results highlighted the functions of PHGDH in mediating the production of serine and its inhibitory effects on megakaryocytic differentiation and PLP generation.

TPO administration lessens thrombocytopenia and suppresses MM progression

After discovering the decrease of platelets induced by excessive serine in the BM microenvironment of MM, we asked whether thrombocytopenia could be improved by the administration of TPO, a critical regulator of megakaryopoiesis and thrombopoiesis [23]. To this end, we next examined the effect of exogenous supply of TPO *in vivo* on thrombocytopenia caused by excessive serine (Fig. 7a). The serine concentration in the serum was elevated in mice fed with high-serine diet compared with control diet, but was reduced in mice with TPO intervention (Fig. 7b). The numbers of MKs and platelets in mice were also restored to higher levels with TPO intervention (Fig. 7c, d). In addition, quantitative imaging analysis revealed enhanced infiltration of tumor cells and tumor burden after feeding with high-serine diet, which

was reduced after the administration of TPO (Fig. 7e, f). Furthermore, the administration of TPO significantly improved the survival of MM mice (Fig. 7g). Together, these results suggest that TPO administration suppresses MM progression and improves the survival of MM mice, at least partially by facilitating megakaryopoiesis and thrombopoiesis.

Discussion

In the present study, we showed that thrombocytopenia correlates with poor prognosis of NDMM patients, especially for those at ISS stage III that are also accompanied with progressive loss of mature MKs. Further un-targeted and targeted metabolic assay showed that the serine level is highly elevated in MM patients with thrombocytopenia. The excessive production of serine is originated from MM cells, while the impact of serine on thrombocytopenia is mainly mediated through the suppression of MK differentiation in the BM and the induction of apoptosis of platelets in the PB. Extrinsic serine intake by SLC38A1 inhibits SVIL expression via SAM, leading to the repression of megakaryopoiesis (Fig. 7h). Finally, inhibition of serine utilization and the pharmacological treatment with TPO restore megakaryopoiesis and the production of platelets, suggesting a promising strategy to improve the therapeutic outcomes of MM.

Earlier studies demonstrated that MM patients have lower platelet levels, which correlate with poor prognosis, although the criteria of thrombocytopenia are defined differently in these studies [4,5,24,25].However, whether thrombocytopenia can be integrated into the prognostic classification systems of MM and the correlation between thrombocytopenia and clinical pathology are still unclear. Here we systematically analyzed the role of thrombocytopenia in

the pathogenesis of MM from the following aspects. First, we discovered that lower platelet numbers are associated with more severe disease outcomes. Approximately, 21.2% of the MM patients have low platelet number ($\leq 100x10^9/L$) accounted. Furthermore, the patients with low platelet counts (7% of total MM patients) suffer from severe life-threatening bleeding, such as gastrointestinal hemorrhage and intracranial hemorrhage (Supplementary Table S8). The data of 1,468 patients from three centers in China showed that thrombocytopenia is much more severe than previously reported [3,26] and clearly merits further attention in the future. The advanced disease stage and the genetic variations are postulated to be responsible for the increased proportion of thrombocytopenia of MM in China. Moreover, we found that the patients with thrombocytopenia correlate with anemia and genetic heterogeneity, including 1q21 gain and TP53 deletion, but it is unclear whether the genetic heterogeneity affects thrombocytopenia and whether myeloid progenitor cells are also affected by the microenvironment of myeloma when the progenitor cells differentiate into erythrocytes. Third, the nutritional conditions and metabolic factors necessary for the survival of residual MK cells in BM are still poorly defined. Previously, we found that the metabolic imbalance of amino acids in BM promotes the proliferation of MM cells [13]. We also revealed the existence of heterogeneous subpopulations of MKs with distinct functions in the human embryos and BM by using single-cell RNA-seq [27,28]. Taken together, our earlier findings suggested that the heterogeneity of MKs may also exist under the pathological conditions of MM. On the one hand, the heterogeneous nature of MKs may explain why the MM patients with poor prognosis have the normal number of platelets. On the other hand, the residual genetically heterogeneous MK cells might require specific nutrients and factors to survive in the BM. But how the different

subpopulations of MKs respond to the microenvironment and then exert their different regulation functions need further investigation. In the present study, we showed that the patients with high serine concentrations in the BM are linked to thrombocytopenia, suggesting that serine might serve as a survival factor for the residual MKs.

MM is characterized by the infiltration of malignant plasma cells into the BM microenvironment where MM cells interact with other cell types to promote MM cell growth and drug resistance [29,30]. Here, we revealed the decrease of MKs and MEPs in MM. Several earlier studies reported that $CD41^{+}CD42d^{+}$ MKs and $CD34^{+}$ stem/progenitor cells are severally impaired due to their interactions with tumor cells, stromal cells or soluble cytokines, leading to the impairment of MK differentiation [31,32]. In this study, we observed increased level of serine in the BM plasma of MM patients with thrombocytopenia. Interestingly, our recent work had shown that PHGDH, the rate-limiting enzyme in serine biosynthesis, promotes proliferation and resistance of MM cells to BTZ by elevating GSH [12]. In the present study, we further demonstrated that PHGDH expression in MM cells is higher than in other cell types and that MM cells are the main source of serine where serine is released to the BMME. Extrinsic serine acts on MKs in the BM and induces apoptosis of platelets in the PB to induce thrombocytopenia in the MM patients. These findings revealed a pathological microenvironment in MM that influences megakaryopoiesis as well as thrombopoiesis and provide potential new targets for therapeutic interventions.

Serine is involved in many critical metabolic processes, including protein biosynthesis, glutathione synthesis, and one-carbon unit metabolism [33,34]. Serine participates in the S-adenosylmethionine cycle through one carbon unit metabolism and provides active methyl

groups for the methylation of proteins and DNA in cells [35]. We found that serine participates in the methionine cycle after entering the cell, promotes the trimethylation of lysine of histone H3, leads to transcriptional inhibition, and silences the expression of target genes. Therefore, inhibiting the catabolism of one-carbon unit of serine may have potential therapeutic significance for preventing thrombocytopenia caused by excessive serine. The differentiation of HSPCs into megakaryocytes is mainly regulated by the TPO signaling pathway and transcription factors includingRUNX1, FLI1, GATA1 and MEIS1, which play important roles in megakaryocyte differentiation [36-38]. In our current study, we found that serine can not only regulate the expression of RUNX1, but also down-regulate SVIL. SVIL is an actin-binding protein associated with cytokinesis [39]. Numerous actin-binding proteins such as non muscle myosin IIA (NMIIA), α-actinin1, and cofilin1 play crucial roles in proplatelet generation [40-42]. However, the role of SVIL in megakaryocyte differentiation has not been reported previously. We found that both SVIL and RUNX1 can promote megakaryocyte differentiation and platelet production. However, in contrast to RUNX1, SVIL is regulated by histone trimethylation mediated by serine release. Whether inhibition of serine metabolism or histone trimethylation can alleviate thrombocytopenia in MM remains to be studied.

The results from our study also pave the way for potential new interventions that target MM from the perspective of abnormal amino-acid metabolism and regulation to effectively improve the survival of patients with MM. Specifically, our present study explored the therapeutic potential in three aspects: the identity of the amino acid (serine), the metabolic enzymes mediating the intake and utilization of serine, and the application of TPO that functions through its receptor MPL (myeloproliferative virus ligand). TPO is widely expressed

on the surface of HSPCs and MKs and stimulates the production and differentiation of megakaryocytes and consequently the expansion of PLTs. Thus, maintaining the normal platelet levels in the MM patients during the treatment may be an effective strategy in the treatment of MM in an individualized manner.

Together, we showed that the degree of thrombocytopenia may assist in the risk stratification of MM and provide new insights into the treatment of newly diagnosed MM patients. The high level of serine may be indicative of myeloma-related thrombocytopenia and may open new avenues for potential new dietary and therapeutic interventions such as serine-restrictive diets and TPO application for MM patients.

Materials and Methods

Patient samples

For the analysis of the correlation of platelet counts and MM progression, a total of 1,468 patients with NDMM were enrolled into the multicenter retrospective study. 1,009 patients diagnosed with MM from the Institute of Hematology and Blood Diseases Hospital, Chinese Academy of Medical Sciences (Tianjin) between 1995 and 2014, 384 from Peking Union Medical College (Beijing) between 2006 and 2017, and 75 from the first and the third Xiangya Hospital, Central South University (Changsha) between 2014 and 2019. For the analysis of the correlation of platelet counts and MKs, the records of BM smears from 24 cases of healthy donors and 98 cases of MM patients were obtained from the Institute of Hematology and Blood Diseases Hospital (Tianjin). 30 BM plasma samples for un-targeted metabonomics analysis were collected from the first and the third affiliated Xiangya Hospital, Central South University

(Changsha). 114 BM plasma samples for targeted metabonomics analysis were from the Institute of Hematology and Blood Diseases Hospital (Tianjin).

5TGM1 mice model

C57Bl/KaLwRijHsd mice of 6 weeks old were purchased from Harlan Laboratories Inc. (Harlan Netherlands BV, The Netherlands). 8-weeks-old mice were inoculated intravenously (IV) with phosphate-buffered saline vehicle (ctrl mice) or 1×10^6 luciferase labeled 5TGM1 cells (5TGM1 mice) and clinical end point was achieved when mice exhibited signs of hindlimb weakness. For the analysis of dynamic changes of MKs, MEPs, CMPs and LSK cells, healthy and myeloma-bearing mice were sacrificed in week 4 and 6 post-inoculation. The progression of the tumors was assessed by using serum analysis of the myeloma-specific IgG2b and bioluminescence imaging (BLI). Briefly, mice were injected intraperitoneally with 15 mg/mL luciferin in PBS at a dose of 150 mg luciferin per kilogram mouse and imaged in weeks 2, 4, 6 or 8 via BLI, followed by an incubation period of 5 minutes. The fluorescence intensity of BLI output was acquired by subtracting the background and analyzed using Living Image Software (PerkinElmer, USA). In the serine intervention study, mice were fed with the control diet and serine-free diet for 1 week before inoculated with 5TGM1cells to develop MM. In the rhTPO intervention study, rhTPO (Peprotech, USA) was injected subcutaneously (SC) from week 2.5 post tumor inoculation for 4 consecutive days (1 μg/mouse/d) [43]. Tumor burden was monitored every 2 weeks until the sacrifice of mice.

MK differentiation

Megakaryocytic differentiation was performed as previously described (21). $CD34^+$ cells were cultured in StemSpan™ SFEM (StemCell Technologies, Canada) supplemented with 1% P/S (Gibco, USA) and cytokines hTPO (50 ng/ml, Peprotech), hIL-3 (20 ng/ml, Peprotech), hSCF (20ng/ml, Peprotech). After 6 days of expansion, cells were transferred to StemSpan™ SFEM supplemented with hTPO (50 ng/mL) and hIL-11 (20 ng/mL) for megakaryocytic differentiation. For cells treated with CM, fresh medium was mixed at a 1:1 ratio with the CM for MK differentiation. For cells treated with amino acids, amino acids were added directly to each well at day 6 of MK differentiation. For MK differentiation of $C\text{-}kit^+$ cells from the control mice, cells were cultured in the presence of 50 ng/mL murine TPO (mTPO, Peprotech) and 20 ng/mL murine SCF to obtain murine MKs.

Metabolomics analysis

Gas chromatography coupled to time-of-flight mass spectrometry (GC-TOFMS) system (Pegasus HT, Leco Corp., St. Joseph, USA) was used to quantify the detected metabolites (Metabo-Profile Biotechnology Co. Ltd, China) [44]. The experimental method was as previously described [13]. Briefly, bucket tables were imported into SIMCA-P 14.0 software (Umetrics AB). Orthogonal partial least squares discriminant analysis (OPLS-DA) was conducted to produce models of "best fit" between the groups of samples. The variable importance in projection (VIP) >1 and fold change (FC) > 1.2 were considered as differential metabolites. Liquid chromatography tandem-mass spectrometry (LC-MS) was used for quantitative analysis of amino acids in the BM plasma from MM patients with normal platelet counts or thrombocytopenia.

$^{13}C_3$-serine and $^{13}C_2$-glycine labeling experiments

$CD34^+$ cells were plated in 10-cm dishes in StemSpan™ SFEM medium. After 6 days of expansion and 3 or 6 days after megakaryocytic differentiation, cells were counted and then cultured in fresh medium supplemented with 100 ng/mL $^{13}C_3$-serine (Yifei Biological Technology Co., Ltd, China) for 4h before metabolite extraction [45]. The time of addition of tracer media was designated as time 0. To mimic the tumor microenvironment of MM, $CD34^+$ cells were cultured with the CM of ARP1 and RPMI-8226 cells on day 6 and subsequently transferred to the CM supplemented with 100 ng/mL $^{13}C_3$-serine on day 9 and day 12 of megakaryocyte differentiation. Cells were washed three times with cold PBS after 4 h of tracing, and the dry pellets were stored at −80 °C. For analysis the release of serine from MM cells, ARP1 cells cultured in fresh medium supplemented with 10 ng/mL $^{13}C_2$-glycine for 2h, 4h, 6h and 8h before supernatant collection. All samples were used for UPLC-QTOFMS analysis (Metabo-Profile Biotechnology Co. Ltd, China).

ATAC-seq (assay for transposase-accessible chromatin using sequencing)

ATAC-seq analysis was performed in differentiated cells treated with or without serine at day 12 of megakaryocytic differentiation (Novogene Biotechnology Co. Ltd, China). ATAC-seq reads were mapped to the hg38 reference genome using bowtie [46]. A p-value less than 0.01 was used to define differentially accessible peaks between control and experimental group. Peaks were displayed using the Integrative Genomics Viewer.

RNA-seq analysis

RNA-seq analysis was performed in differentiated cells with various treatments at day 12 of megakaryocytic differentiation, including cells treated with ARP1 CM or with serine. Total RNA was isolated using Trizol reagent following manufacturer's protocol. The mRNA is fragmented into short fragments and cDNA is synthesized using the mRNA fragments as templates. The short fragments were then purified and connected with adapters, and the transcriptome data of those cells were profiled by using a BGISEQ-500 (Beijing Genomics Institute at Wuhan, China). After quality control (QC) analysis was conducted, the read counts were generated by aligning the human genome assembly. FPKM (Reads Per Kilobase of exon model per Million mapped reads) values were generated using the edgeR package. Differentially expressed genes were identified if they had a p value < 0.05 and FC $>$ 1.2 between two groups.

Statistical analysis

Relations between platelet counts and discrete variables were tested by using the chi-square or Fisher's exact test. Kaplan-Meier survival curves were evaluated by using a two-sided log-rank test. Data were analyzed using a student unpaired t test for the comparison of two groups, paired t test for the comparison of paired samples, and one-way analysis of variance (ANOVA) for the comparison of more than two groups. Data are presented as mean ± standard error of the mean (SEM) as indicated. $p < 0.05$ was considered significant.

Study approval

All animal experiments were conducted in accordance with a protocol approved by the

Institutional Animal Care and Use Committee of Central South University (approval number: D2021016). All human BM samples were obtained with written informed consent from patients or their guardians prior to participation in the study. The experimental protocol was approved by the Institutional Review Board of all participating hospitals.

Additional details are described in Supplemental Materials and Methods (Supplementary data).

Declarations

Data availability

The datasets for RNA sequence analysis and other datasets analyzed during the present study are available from the corresponding author upon reasonable requests.

Acknowledgements

We thank Prof. Yuhuan Zheng (West China Center of Medical Sciences, Sichuan, China) for providing luciferase-labeled 5TGM1 cell line. We thank Wenying Yu and Weichao Fu for technical assistance with flow cytometry. We thank Ting Chen, and Wanzhu Yang for technical supports with confocal microscope. We also thank professor Rushi Liu and Kaiqun Ren from Hunan Normal University School of Medicine for their assistance with bioluminescence imaging. Thanks to the Animal Center of Hunan Normal University School of Medicine for providing the experimental platform. This work was supported by the Ministry of Science and Technology of China (2018YFA0107800); National Natural Science Foundation of China (82130006, 82125003, 81974010); Natural Science Foundation of Hunan Province (2021JJ3089, 2020WK2006), Strategic Priority Research Program of Central South University (ZLXD2017004), CAMS Innovation Fund for Medical Sciences (CIFMS) (2021-I2M-1-073), SKLEH-Pilot Research Grant (ZK21-05), China Postdoctoral Science Foundation (2021M703631), Postdoctoral Science Foundation of Central South University (22021101228).

Author contributions

Contribution: W.Z and J.Z conceived of and designed the experiments; C.K, M.X, J.Z, C.H, B.M, J.X, X.W, J.G and Y.Z performed the experiments; C.K, M.X, C.L, J.Z, C.H, B.M, Z.L, X.W and X.F analyzed the data; G.A, P.S, L.Q, J.L, Y.S, and Y.H provided critical materials; W.Z , J.Z and C.K wrote the manuscript and all authors edited the manuscript.

Competing interests

The authors declare no competing financial interests.

Correspondence：Wen Zhou, Cancer Research Institute, Central South University, Changsha, China, 410078, e-mail: wenzhou@csu.edu.cn; Jiaxi Zhou, State Key Laboratory of Experimental Hematology, National Clinical Research Center for Blood Diseases, Chinese Academy of Medical Sciences & Peking Union Medical College, Tianjin China, 300020,e-mail: zhoujx@ihcams.ac.cn.

References

1. Liu, J.*, et al.* Incidence and mortality of multiple myeloma in China, 2006-2016: an analysis of the Global Burden of Disease Study 2016. *J Hematol Oncol* **12**, 136 (2019).
2. Cowan, A.J.*, et al.* Diagnosis and Management of Multiple Myeloma: A Review. *JAMA* **327**, 464-477 (2022).
3. Kyle, R.A.*, et al.* Review of 1027 patients with newly diagnosed multiple myeloma. *Mayo Clin Proc* **78**, 21-33 (2003).
4. Al Saleh, A.S.*, et al.* Hematopoietic score predicts outcomes in newly diagnosed multiple myeloma patients. *Am J Hematol* **95**, 4-9 (2020).
5. Kaneko, M.*, et al.* Simple prognostic model for patients with multiple myeloma: a single-center study in Japan. *Ann Hematol* **81**, 33-36 (2002).
6. Greipp, P.R.*, et al.* International staging system for multiple myeloma. *J Clin Oncol* **23**, 3412-3420 (2005).
7. Machlus, K.R. & Italiano, J.E., Jr. The incredible journey: From megakaryocyte development to platelet formation. *J Cell Biol* **201**, 785-796 (2013).
8. Li, W.*, et al.* Thrombocytopenia in MDS: epidemiology, mechanisms, clinical consequences and novel therapeutic strategies. *Leukemia* **30**, 536-544 (2016).
9. Shahrabi, S., Behzad, M.M., Jaseb, K. & Saki, N. Thrombocytopenia in leukemia: Pathogenesis and prognosis. *Histol Histopathol* **33**, 895-908 (2018).
10. Gao, A.*, et al.* Bone marrow endothelial cell-derived interleukin-4 contributes to

623 thrombocytopenia in acute myeloid leukemia. *Haematologica* **104**, 1950-1961 (2019).
624 11. Shastri, A., Will, B., Steidl, U. & Verma, A. Stem and progenitor cell alterations in
625 myelodysplastic syndromes. *Blood* **129**, 1586-1594 (2017).
626 12. Wu, X*., et al.* Phosphoglycerate dehydrogenase promotes proliferation and bortezomib
627 resistance through increasing reduced glutathione synthesis in multiple myeloma. *Br J*
628 *Haematol* **190**, 52-66 (2020).
629 13. Jian, X*., et al.* Alterations of gut microbiome accelerate multiple myeloma progression by
630 increasing the relative abundances of nitrogen-recycling bacteria. *Microbiome* **8**, 74 (2020).
631 14. Murphy, A.J*., et al.* Cholesterol efflux in megakaryocyte progenitors suppresses platelet
632 production and thrombocytosis. *Nat Med* **19**, 586-594 (2013).
633 15. Ye, J.Y*., et al.* Serotonin enhances megakaryopoiesis and proplatelet formation via p-Erk1/2
634 and F-actin reorganization. *Stem Cells* **32**, 2973-2982 (2014).
635 16. Pietras, N.M. & Pearson-Shaver, A.L. Immune Thrombocytopenic Purpura. in *StatPearls*
636 (Treasure Island (FL), 2022).
637 17. Rajkumar, S.V. Multiple myeloma: 2020 update on diagnosis, risk-stratification and
638 management. *Am J Hematol* **95**, 548-567 (2020).
639 18. Gooding, S*., et al.* Transcriptomic profiling of the myeloma bone-lining niche reveals BMP
640 signalling inhibition to improve bone disease. *Nat Commun* **10**, 4533 (2019).
641 19. Yang, Y*., et al.* Integrated Biophysical and Biochemical Signals Augment Megakaryopoiesis and
642 Thrombopoiesis in a Three-Dimensional Rotary Culture System. *Stem Cells Transl Med* **5**, 175-
643 185 (2016).
644 20. Lebois, M. & Josefsson, E.C. Regulation of platelet lifespan by apoptosis. *Platelets* **27**, 497-504
645 (2016).
646 21. Qiao, J*., et al.* Imbalanced expression of Bcl-xL and Bax in platelets treated with plasma from
647 immune thrombocytopenia. *Immunol Res* **64**, 604-609 (2016).
648 22. Kimball, A.S*., et al.* The Histone Methyltransferase Setdb2 Modulates Macrophage Phenotype
649 and Uric Acid Production in Diabetic Wound Repair. *Immunity* **51**, 258-271 e255 (2019).
650 23. Kimura, S., Roberts, A.W., Metcalf, D. & Alexander, W.S. Hematopoietic stem cell deficiencies
651 in mice lacking c-Mpl, the receptor for thrombopoietin. *Proc Natl Acad Sci U S A* **95**, 1195-1200
652 (1998).
653 24. Ludwig, H*., et al.* Bendamustine-bortezomib-dexamethasone is an active and well-tolerated
654 regimen in patients with relapsed or refractory multiple myeloma. *Blood* **123**, 985-991 (2014).
655 25. Rodon, P*., et al.* Multiple myeloma in elderly patients: presenting features and outcome. *Eur J*
656 *Haematol* **66**, 11-17 (2001).
657 26. Kyle, R.A. Multiple myeloma: review of 869 cases. *Mayo Clin Proc* **50**, 29-40 (1975).
658 27. Wang, H*., et al.* Decoding Human Megakaryocyte Development. *Cell Stem Cell* **28**, 535-549
659 e538 (2021).
660 28. Liu, C*., et al.* Characterization of Cellular Heterogeneity and an Immune Subpopulation of
661 Human Megakaryocytes. *Adv Sci (Weinh)* **8**, e2100921 (2021).
662 29. Lomas, O.C., Tahri, S. & Ghobrial, I.M. The microenvironment in myeloma. *Curr Opin Oncol* **32**,
663 170-175 (2020).
664 30. Garcia-Ortiz, A*., et al.* The Role of Tumor Microenvironment in Multiple Myeloma
665 Development and Progression. *Cancers (Basel)* **13**(2021).
666 31. Bruns, I*., et al.* Multiple myeloma-related deregulation of bone marrow-derived CD34(+)

hematopoietic stem and progenitor cells. *Blood* **120**, 2620-2630 (2012).
32. Zhou, L.*, et al.* Reduced SMAD7 leads to overactivation of TGF-beta signaling in MDS that can be reversed by a specific inhibitor of TGF-beta receptor I kinase. *Cancer Res* **71**, 955-963 (2011).
33. Locasale, J.W. Serine, glycine and one-carbon units: cancer metabolism in full circle. *Nat Rev Cancer* **13**, 572-583 (2013).
34. Amelio, I., Cutruzzola, F., Antonov, A., Agostini, M. & Melino, G. Serine and glycine metabolism in cancer. *Trends Biochem Sci* **39**, 191-198 (2014).
35. Maddocks, O.D., Labuschagne, C.F., Adams, P.D. & Vousden, K.H. Serine Metabolism Supports the Methionine Cycle and DNA/RNA Methylation through De Novo ATP Synthesis in Cancer Cells. *Mol Cell* **61**, 210-221 (2016).
36. Almazni, I., Stapley, R. & Morgan, N.V. Inherited Thrombocytopenia: Update on Genes and Genetic Variants Which may be Associated With Bleeding. *Front Cardiovasc Med* **6**, 80 (2019).
37. Balduini, C.L., Melazzini, F. & Pecci, A. Inherited thrombocytopenias-recent advances in clinical and molecular aspects. *Platelets* **28**, 3-13 (2017).
38. Wang, H.*, et al.* MEIS1 Regulates Hemogenic Endothelial Generation, Megakaryopoiesis, and Thrombopoiesis in Human Pluripotent Stem Cells by Targeting TAL1 and FLI1. *Stem Cell Reports* **10**, 447-460 (2018).
39. Smith, T.C.*, et al.* Supervillin binding to myosin II and synergism with anillin are required for cytokinesis. *Mol Biol Cell* **24**, 3603-3619 (2013).
40. Begonja, A.J.*, et al.* FlnA binding to PACSIN2 F-BAR domain regulates membrane tubulation in megakaryocytes and platelets. *Blood* **126**, 80-88 (2015).
41. Kunishima, S.*, et al.* ACTN1 mutations cause congenital macrothrombocytopenia. *Am J Hum Genet* **92**, 431-438 (2013).
42. Bender, M.*, et al.* ADF/n-cofilin-dependent actin turnover determines platelet formation and sizing. *Blood* **116**, 1767-1775 (2010).
43. Inagaki, K.*, et al.* Induction of megakaryocytopoiesis and thrombocytopoiesis by JTZ-132, a novel small molecule with thrombopoietin mimetic activities. *Blood* **104**, 58-64 (2004).
44. Qiu, Y.*, et al.* Serum metabolite profiling of human colorectal cancer using GC-TOFMS and UPLC-QTOFMS. *J Proteome Res* **8**, 4844-4850 (2009).
45. Newman, A.C., Labuschagne, C.F., Vousden, K.H. & Maddocks, O.D.K. Use of (13)C3(15)N1-Serine or (13)C5(15)N1-Methionine for Studying Methylation Dynamics in Cancer Cell Metabolism and Epigenetics. *Methods Mol Biol* **1928**, 55-67 (2019).
46. Langmead, B., Trapnell, C., Pop, M. & Salzberg, S.L. Ultrafast and memory-efficient alignment of short DNA sequences to the human genome. *Genome Biol* **10**, R25 (2009).

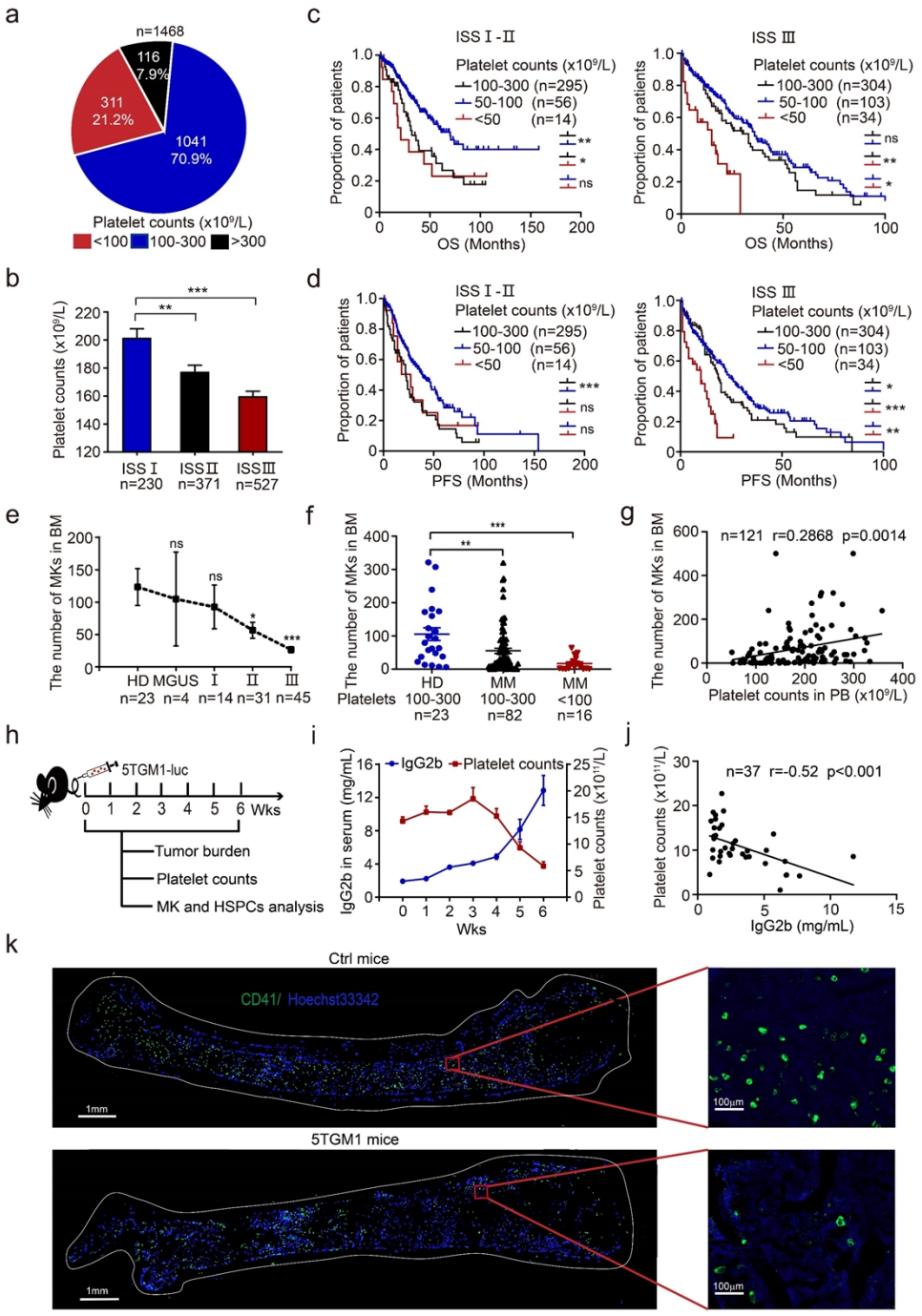

706

707 **Figure 1. Thrombocytopenia is linked to poor prognosis in MM patients.** (**a**) Assessment of platelet counts in

708 newly diagnosed MM (NDMM) patients (n = 1,468). Three groups were defined as follows: patients with normal-

709 platelet counts (100-300×10^9/L, n = 1041), high-platelet counts (> 300×10^9/L, n = 116) and low-platelet counts

710 (≤100×10^9/L, n = 311). (**b**) Platelet counts in PB (peripheral blood) of NDMM patients with different ISS stage

711 (mean ± SEM, nISS I = 230, nISS II = 371; nISS III = 527). (**c** and **d**) Kaplan-Meier analyses of overall survival

(OS) (**c**) and progression free survival (PFS) (**d**) in NDMM patients with normal-platelet counts (100-300×10^9/L), low-platelet counts (50-100×10^9/L) and low-platelet counts (< 50×10^9/L). (**e**) The number of MKs in BM aspirate smears derived from healthy donors (HD), MGUS (monoclonal gammopathy of undetermined significance) and NDMM patients with different ISS stage (nHD = 23, nMGUS=4, nISS I = 14, nISS II = 31; nISS III = 45). (**f**) The number of MKs in BM aspirate smears derived from HD and MM patients with normal-platelet counts and low-platelet counts (mean ± SEM, nHD = 23, nplatelet (normal) = 82, nplatelet (low) = 16). (**g**) Assessment of the correlation between platelet counts and numbers of MKs in BM (n = 121). (**h**) Schematic diagram of the experimental design to detect platelet counts, tumor burden and the proportion of LSKs, CMPs, and MEP in 5TMG1 MM mouse model. (**i**) Dynamic changes of IgG2b levels and platelet counts during MM progression. IgG2b level was detected by using ELISA assay. Peripheral platelet counts were measured with haematologyanalyser (n = 6). (**j**) Assessment of the correlation between IgG2b levels and platelet counts (n = 37). (**k**) Representative images of immunofluorescence analysis for MKs staining using CD41-FITC antibody (Green) and Hoechst 33342 (Blue) in the BM of control mice and MM mice. Top, normal numbers of MKs in control mice; bottom, decreased numbers of MKs in MM mice. *p < 0.05, **p < 0.01, ***p < 0.001, ns: not significant (p > 0.05). p values were calculated using Log-rank test (**c**, **d**). p values were calculated using one-way ANOVA (**b**, **e**, **f**).

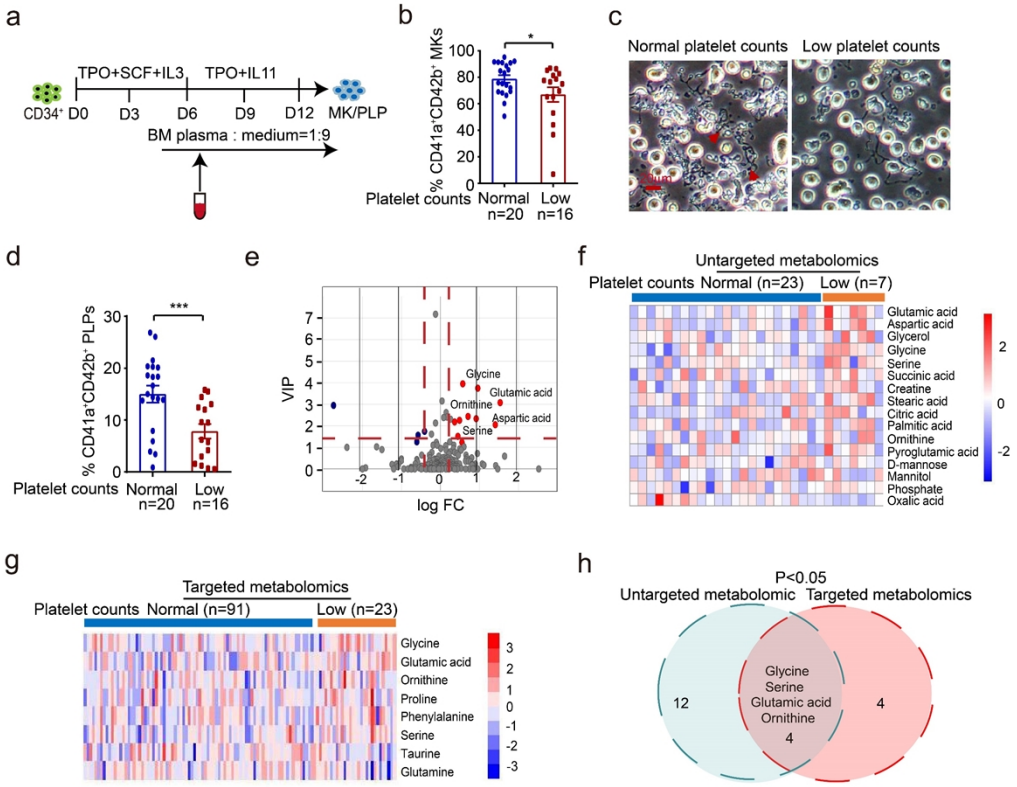

Figure 2. Serine is upregulated in BM and linked to thrombocytopenia in MM. (**a**) Schematic diagram showing megakaryocytic differentiation of $CD34^+$ cells treated with BM plasma derived from MM patients with or without thrombocytopenia. (**b**) Flow cytometry analysis of the percentage of $CD41a^+CD42b^+$ cells at day 12 of megakaryocytic differentiation with BM plasma treatment (mean ± SEM, nplatelet (normal) = 20, nplatelet (low) = 16). (**c**) Phase-contrast images of proplatelet formation at day 12 from $CD34^+$ cells with BM plasma treatment (scale bar, 20μm). (**d**) Generation of $CD41a^+CD42b^+$ PLPs at day 12 of $CD34^+$ cells with BM plasma treatment (mean ± SEM, nplatelet (normal) = 20, nplatelet (low) = 16). (**e**) Volcano plot of differential metabolites in BM plasma between MM patients with normal-platelet counts (n = 23) and patients with low-platelet counts (n = 7) by using with un-targeted metabolomics. Significantly upregulated metabolites are represented as 'red' dots, and downregulated metabolites are represented as 'blue' dots. (**f**) Heat maps of the 16 differential metabolites in BM plasma between MM patients with normal platelet counts and with low platelet counts. (**g**) Heatmaps of the 8 differential amino acids in BM plasma between MM patients with normal platelet counts (n = 91) and patients with

low platelet counts (n = 23) revealed with targeted metabolomics. (**h**) Venn diagram of un-targeted metabolomics and targeted metabolomics. *p < 0.05. p values were calculated using two-tailed unpaired Student's t-tests (**b**, **d**).

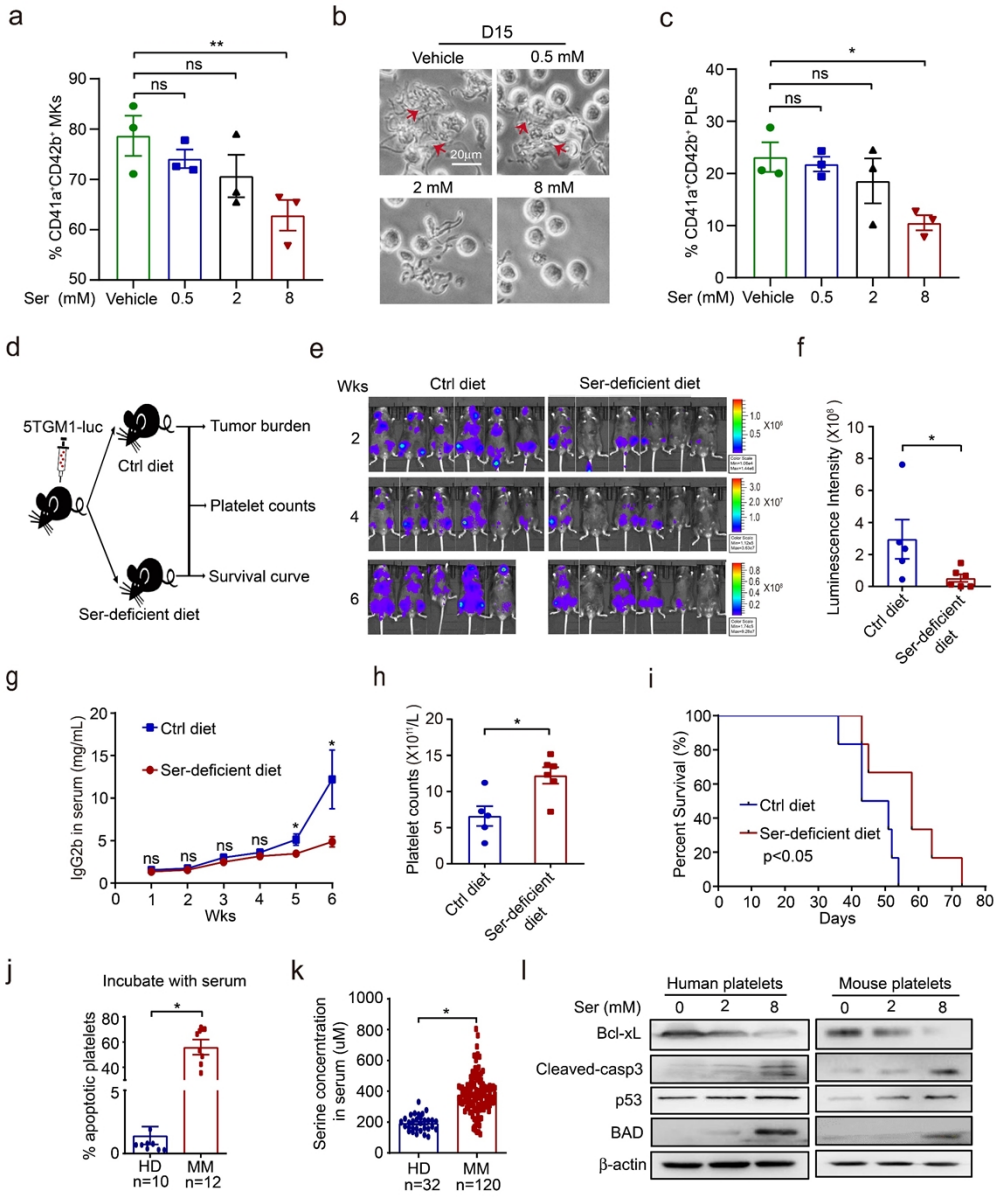

Figure 3. Serine inhibits megakaryopoiesis and thrombopoiesis *in vitro* and *in vivo*. (**a**) The production of $CD41a^+CD42b^+$ MKs of $CD34^+$ cells with indicated concentration of serine (mean ± SEM, n = 3 for each group). (**b**) Phase-contrast images of proplatelet formation at day 12 from $CD34^+$ cells with indicated concentrations of serine. (**c**) The production of $CD41a^+CD42b^+$ PLPs of $CD34^+$ cells with indicated concentrations of serine (mean ± SEM, n = 3 for each group). (**d**) Schematic diagram of the experimental design to detect tumor burden,

platelet counts and the survival in 5TMG1 MM mouse model fed with the control diet or serine-deficient diet (n = 6 per group). (**e**) Tumor-associated luminescence intensity in live 5TGM1 MM mice fed with the control diet or serine-deficient diet. (**f**) Quantification of luminescence intensity in 5TGM1 MM mice fed with the control diet or serine-deficient diet at 2, 4, 6 weeks (mean ± SEM). (**g**) The concentrations of IgG2b in mouse serum as detected with ELISA. (**h**) The number of platelet counts in PB in 5TGM1 MM mice fed with the control diet or serine-deficient diet. (**i**) The survival curves of 5TGM1 MM mice fed with the control diet or serine-deficient diet. (**j**) The apoptosis rate of platelets derived from HD incubated with serum from HD or MM patients. (**k**) The level of serine in serum from HD or MM patients as revealed with targeted metabolomics. (**l**) Western blot analysis of BCL-xL, C-caspase3, p53 and BAD expression in platelets derived from HD or control mice treated with indicated concentration of serine. *p< 0.05, **p< 0.01, ns: not significant (p > 0.05). p values were calculated using one-way ANOVA (**a**, **c**). p values were calculated using two-tailed unpaired Student's t-tests (**f**, **h**, **j**, **k**). p value was calculated using Log-rank test (**i**).

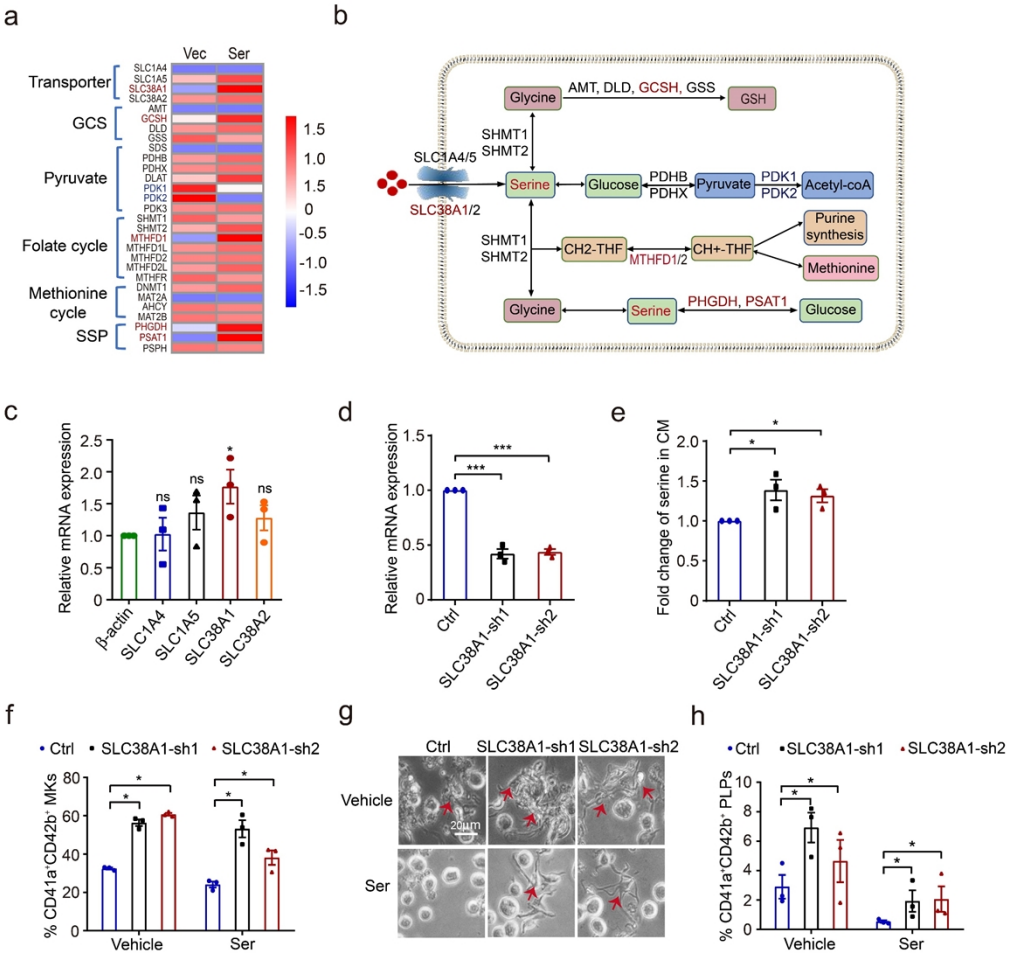

Figure 4. Serine intake is mediated by SLC38A1. (**a**) The expression profile of serine metabolism-related genes in MKs cultured with vehicle or excessive serine. (**b**) Schematics of serine metabolism. (**c**) Assessment of mRNA expression of serine transporters in differentiated cells treated with vehicle or excessive serine at day 12. (**d**) The mRNA level of SLC38A1 in $CD34^+$ cells containing control and SLC38A1 shRNAs as detected with qPCR analysis. (**e**) The concentration of extracellular serine in $CD34^+$ cells containing control and SLC38A1 shRNAs. (**f**) Flow cytometry analysis of the percentage of $CD41a^+CD42b^+$ MKs from $CD34^+$ cells with SLC38A1 knockdown exposed to serine. (**g**) Representative images of proplatelet formation from MKs from $CD34^+$ cells with SLC38A1 knockdown exposed to vehicle or serine. (**h**) Generation of $CD41a^+CD42b^+$ PLPs at day 12 from $CD34^+$ cells with SLC38A1 knockdown exposed to vehicle or serine. *p< 0.05, ***p< 0.001, ns: not significant (p > 0.05). p values were calculated using one-way ANOVA.

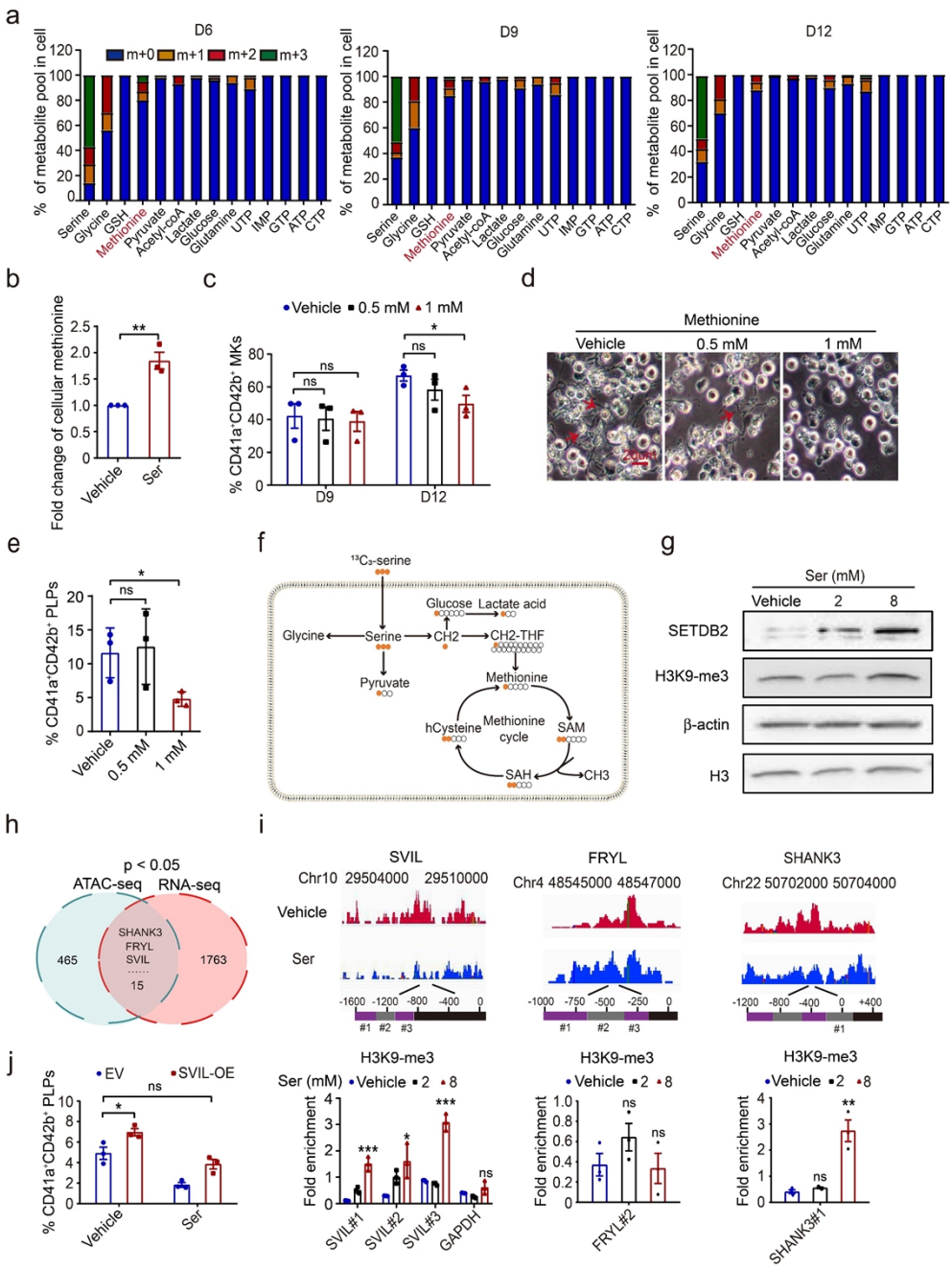

Figure 5. Serine downregulates Supervillin via S-adenosyl-methionine-mediated tri-methylation of H3K9. (**a**) The metabolic flux of $^{13}C_3$ serine in $CD34^+$ cells undergoing MK differentiation. (**b**) The level of cellular methionine in differentiated cells at day 12. (**c**) Generation of $CD41a^+CD42b^+$ MKs of $CD34^+$ cells with indicated concentrations of methionine. (**d**) Phase-contrast images of proplatelet formation at day 12 from $CD34^+$ cells treated with indicated concentrations of methionine. (**e**) Generation of $CD41a^+CD42b^+$ PLPs from $CD34^+$ cells with indicated concentrations of methionine. (**f**) Schematics of serine metabolism in MKs. (**g**) Western blots of SETDB2, β-actin,

H3K9-me3 and H3 in differentiated cells cultured with vehicle or serine at day 12. (**h**) Venn diagram of downregulated genes in both ATAC-seq and RNA-seq analyses. (**i**) Peaks of the promoter of SVIL, FRYL and SHANK3 and the binding of H3K9-me3 to the promoters of the three genes in differentiated cells cultured with vehicle or serine at day 12, as revealed with ATAC-seq and ChIP-qPCR, respectively. (**j**) Generation of $CD41a^{+}CD42b^{+}$ PLPs from $CD34^{+}$ cells with overexpression of SVIL exposed to serine. *p< 0.05, **p< 0.01. p values were calculated using two-tailed unpaired Student's t-tests (**b**). p values were calculated using one-way ANOVA (**c**, **e**, **i**, **j**).

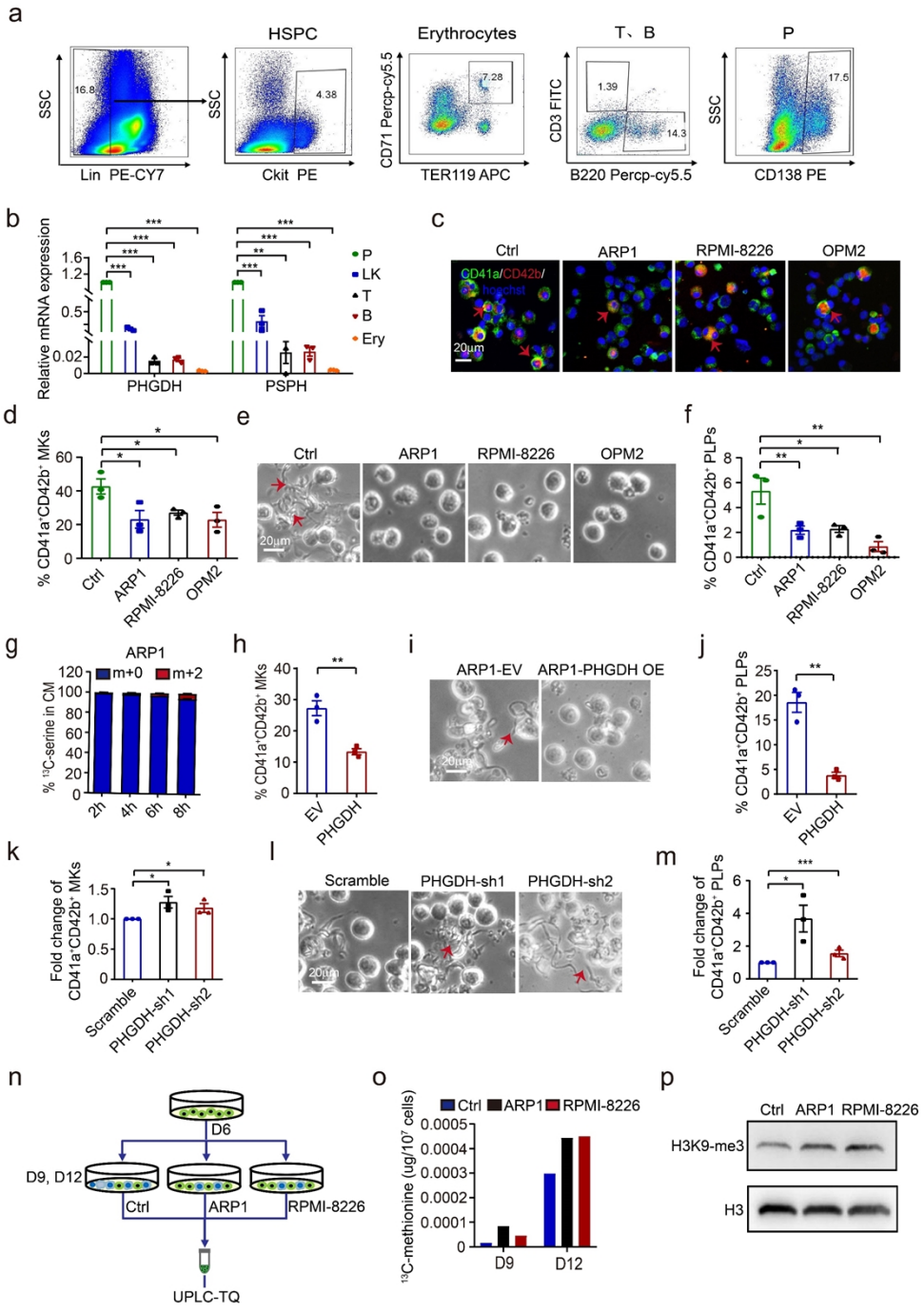

784

785 **Figure 6. Serine accumulated in the BM microenvironment is released from myeloma cells.** (**a**) Representative

786 plots for the isolation of HSPCs, erythrocytes, T cell, B cell and plasma cells from the BM microenvironment of

787 5TGM1 MM mouse. (**b**) Relative mRNA levels of PHGDH and PSPH were detected in HSPCs, erythrocytes, T cell,

788 B cell and plasma cells by using qPCR. (**c**) Representative images of IF for MKs stained with FITC-CD41a and

789 APC-CD42b in differentiated cells treated with or without the CM. (**d**) Flow cytometry analysis of the percentage

of $CD41a^+CD42b^+$ cells at day 9 and 12 of megakaryocytic differentiation with or without the CM treatment. (**e**) Phase-contrast images of proplatelet formation at day 12 from $CD34^+$ cells with or without the CM treatment (scale bar, 20μm). (**f**) Generation of $CD41a^+CD42b^+$ PLPs at day 12 of $CD34^+$ cells with or without CM treatment. (**g**) ^{13}C-labeled serine in the CM from ARP1 cells treated with $^{13}C_2$ glycine. (**h**) Flow cytometry analysis of the percentage of $CD41a^+CD42b^+$ MKs from $CD34^+$ cells treated with CM derived from ARP1-EV and ARP1-PHGDH cells. (**i**) Representative images of proplatelet formation from MKs treated with CMs derived from ARP1-EV and ARP1-PHGDH cells. (**j**) Generation of $CD41a^+CD42b^+$ PLPs at day 12 from $CD34^+$ cells treated with CM derived from ARP1-EV and ARP1-PHGDH cells. (**k**) Flow cytometry analysis of the percentage of $CD41a^+CD42b^+$ MKs from $CD34^+$ cells treated with ARP1-PHGDH-sh1 CM and ARP1-PHGDH-sh2 CM. (**l**) Representative images of proplatelet formation from MKs treated with ARP1-PHGDH-sh1 CM and ARP1-PHGDH-sh2 CM. (**m**) Generation of $CD41a^+CD42b^+$ PLPs at day 12 from $CD34^+$ cells treated with ARP1-PHGDH-sh1CM and ARP1-PHGDH-sh2 CM. (**n**) Schematics of the serine metabolic flux experiments in CM from MM cells. (**o**) Levels of ^{13}C-methionine in cells after incubated with the CM of ARP1 cells and RPMI-8226 cells with $^{13}C_3$-serine for 4 h. (**p**) Western blot analysis of H3K9-me3 in cells at day 12 treated with control or CM from ARP1 cells and RPMI-8226 cells. *p< 0.05, **p< 0.01. p values were calculated using two-tailed unpaired Student's t-tests (**h**, **j**). p values were calculated using one-way ANOVA (**b**, **d**, **f**, **k**, **m**).

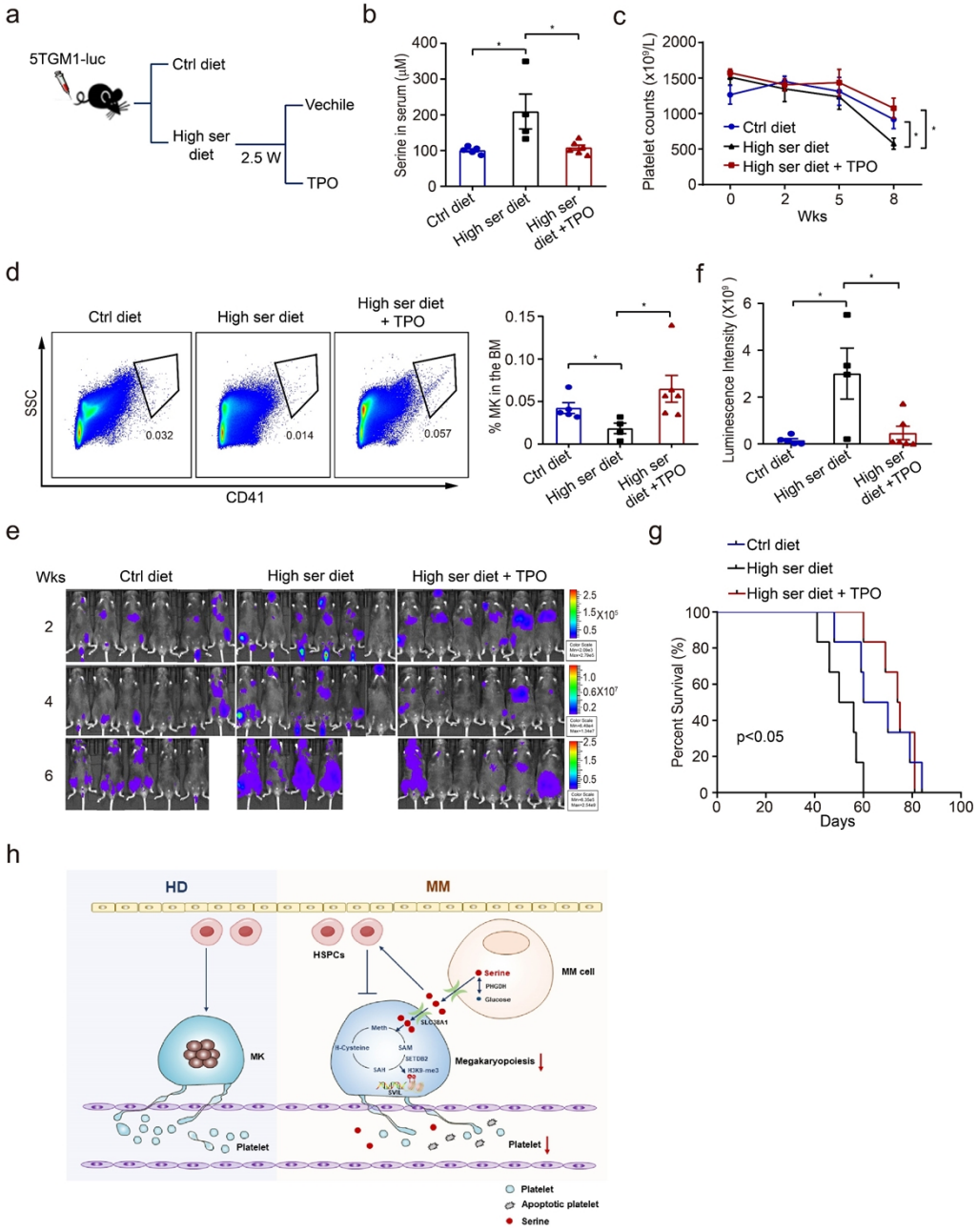

806

807 **Figure 7. TPO administration lessens thrombocytopenia and suppresses MM progression.** (**a**) Schematic

808 diagram of 5TGM1 mice fed with the control diet (n = 6), high-serine diet (n = 6) or high-serine diet plus TPO

809 intervention (2 mg/kg) (n = 6). (**b**) Serum serine concentrations in 5TGM1 mice fed with the indicated diets with

810 BSA or TPO intervention. (**c**) Dynamic changes of platelet counts in PB of 5TGM1mice fed with the indicated diets

811 with BSA or TPO intervention. (**d**) The percentage of MKs in BM cells of 5TGM1 mice fed with the indicated diets

812 with BSA or TPO intervention as revealed with flow cytometry analysis. (**e**) Live imaging of the tumor-associated

luminescence intensity of 5TGM1 MM mice fed with the control diet, high-serine diet or high-serine diet plus TPO for 2, 4, or 6 weeks. (**f**) Quantification of tumor-associated luminescence intensity in the 5TGM1 MM mice cohorts shown in panel e (mean ± SEM). (**g**) The survival curves of 5TGM1 MM mice fed with the control or high-serine diet with or without TPO. (**h**) The working model of this study. *$p < 0.05$. p values were calculated using Log-rank test (**g**). p values were calculated using one-way ANOVA (**b**, **c**, **d**, **f**).

835 **Table 1. The correlation of platelet count and clinical characteristics of MM**

Patients' Characteristics	Low platelet count (n=311) (n/N×100%)	Normal platelet count (n=1041) (n/N×100%)	High platelet count (n=116) (n/N×100%)	p-value (low vs. normal)
Age (y)	60	59	57	0.246
Sex				0.171
Male	197/311 (63.3)	638/1041 (61.3)	62/116 (53.4)	
Female	114/311 (36.7)	403/1041 (38.7)	54/116 (46.6)	
ISS stage				0.000**
I	30/233 (12.9)	177/816 (21.7)	22/84 (26.2)	
II	64/233 (27.5)	280/816 (34.3)	28/84 (33.3)	
III	139/233 (59.6)	358/816 (44)	34/84 (40.5)	
DS stage				0.002**
I	8/279 (2.9)	65/889 (7.3)	8/97(8.2)	
II	18/279 (6.5)	97/889 (10.9)	15/97(15.5)	
III	253/279 (90.6)	727/889 (81.8)	74/97(76.3)	
Plasma cells in BM (%)	40.1	32.8	24.3	0.000***
Median Calcium (mmol/L)	2.32	2.34	2.3	0.743
Renal dysfunction	67/282 (23.8)	195/911 (21.4)	19/99 (19.2)	0.573
Median Hb (g/L)	73.7	93.4	95.3	0.000***
Median LDH (U/L)	221	175	163	0.000***
1q21 gain				0.004**
No	33/113 (29.2)	205/452 (45.4)	29/46 (63)	
Yes	80/113 (70.8)	247/452 (54.6)	17/46 (37)	
TP53 deletion				0.037*
No	94/122 (77)	435/522 (83.3)	50/54 (92.6)	
Yes	28/122 (23)	87/522 (16.7)	4/54 (7.4)	
IgH translocation				0.459
No	45/120 (37.5)	218/498 (43.8)	22/52 (42.3)	
Yes	75/120 (62.5)	280/498 (56.2)	30/52 (57.7)	

Abbreviations: DS stage: Durie-Salmon stage; ISS: International Staging System; FISH, fluorescence in situ hybridization; LDH, lactate dehydrogenase; y, years. Hb: hemoglobin; Renal dysfunction: Creatinine level > 2.0 mg/dL; 1q21 gain: FISH 1q21 gain in ≥10% of cells; TP53 deletion: FISH TP53 deletion in ≥10% of cells; FISH IgH translocation in ≥10% of cells; OS: overall survival; PFS: progression-free survival; all MM patients were newly diagnosed. *$p < 0.05$, **$p < 0.01$, ***$p < 0.001$. The correlations of platelet counts with clinical characteristics were measured using the chi-square test.

Supplementary Files

This is a list of supplementary files associated with this preprint. Click to download.

- SupplementaryTableS1relatedtoFigure1.docx
- SupplementaryTableS2relatedtoFigure1.docx
- SupplementaryTableS3relatedtoFigure2.docx
- SupplementaryTableS4relatedtoFigure4.xlsx
- SupplementaryTableS5relatedtoFigure5.xls
- SupplementaryTableS6relatedtoFigure5.xls
- SupplementaryTableS7relatedtoSupplementarydata.docx
- SupplementaryTableS8relatedtoDiscussion.docx